

The influence of IGF-I and Emdogain on the behavior of dental epithelial cells in a three-dimensional scaffold model

Maria Johanna Jacoba Heezen¹, Weibo Zhang², Sara Rudolph², X. Frank Walboomers¹, Pamela C. Yelick²

¹Radboud University Medical Center, Radboud Institute for Molecular Life Sciences, Department of Dentistry – Regenerative Biomaterials, Philips van Leydenlaan 25, 6525EX Nijmegen, the Netherlands

²Division of Craniofacial and Molecular Genetics, Department of Orthodontics, Tufts University School of Dental Medicine, Boston, Massachusetts 02111, United States of America

Abstract

AIM: Tooth decay and associated periodontal disease remain the most common chronic diseases in current society. In the future, individually tailored, more effective therapeutic treatment options could be provided through the application of tissue engineering and regenerative medicine and dentistry (TERMD) approaches. A relevant finding is the potential of both dental mesenchymal and dental epithelial cells to regenerate mineralized dentin and enamel tissues, respectively.

MATERIALS AND METHODS: In the current study, a multi-layered, bioengineered tooth bud model was assembled by combining human dental mesenchymal (hDM) and porcine dental epithelial cells (pDE). The hDM cells were seeded onto poly (epsilon-caprolactone)/poly (lactide-co-glycolide) (PCL/PLGA) wet electro-spun scaffolds overlayed with confluent pDE cell sheet harvested from thermo-reversible tissue culture plates. The so-formed multi-layered bioengineered tooth bud was then used to study the mineralization potential of the dental cells in *in vitro* culture. It was hypothesized that the addition of the in media soluble factors Insulin-like growth factor 1 (IGF-I) and the extracellular matrix derivate Emdogain (EMD) would result in enhanced differentiation and mineralized dental tissue formation.

RESULTS: Scanning Electron morphological observation was used to characterize scaffolds porosity. Histological and immunofluorescent analyses confirmed the localization of hDM cells inside the scaffold, an intact pDE cell sheet, and the presence of beta-integrin 1-positive cell-cell junctions connecting the two. Scanning Electron Microscopy showed that EMD, in particular, enhanced the mineralization potential of pDE cells. qRT-PCR analyses showed that both EMD and IGF-1 significantly enhanced the expression of Ameloblastin (AMBN), reflecting pDE cell differentiation.

CONCLUSION: In conclusion, these results proved the hypothesis that both EMD and IGF-1 should be considered for their utility in preclinical dental tissue engineering approaches.

KEYWORDS: Tissue engineering; Dental epithelial/mesenchymal cells; scaffold; IGF-1; Emdogain

Citation: Heezen, M et al. (2022) The influence of IGF-I and Emdogain on the behavior of dental epithelial cells in a three-dimensional scaffold model
Dentistry 3000. 1:a001 doi:10.5195/d3000.2022.258
Received: October 21, 2021
Accepted: April 23, 2022
Published: July 8, 2022
Copyright: ©2022 Heezen, M et al. This is an open access article licensed under a Creative Commons Attribution Work 4.0 United States License.
Email: Pamela.Yelick@tufts.edu
Frank.Walboomers@radboudumc.nl

Introduction

Tooth decay remains the most common chronic disease in modern-

day society. According to a recent systematic analysis for the Global Burden of Disease (including data from 195 countries worldwide), over

3.5 billion people are affected by untreated oral diseases [1] that often lead to complete or partial tooth loss as well as systemic diseases.

Prevention and tooth replacement therapies are the current solutions for these problems [2], for example using proper oral hygiene and partial or complete dentures, bridges, crowns and dental implants. Tissue engineering and regenerative medicine and dentistry (TERMD) approaches, used as future therapeutic options to treat oral diseases, could provide the means for living dental tissue regeneration, thus providing individuals with restored comfort and function of their masticatory system adapted to their specific needs [3].

Prior studies in dental tissue engineering have shown that interactions between dental mesenchymal (i.e. the dentin forming odontoblasts) and ectodermal (i.e. the enamel forming ameloblasts) cells are a prerequisite to initiating both dental cell differentiation and mineralization processes. Especially, epithelial cells were proven not to grow and differentiate without the presence of supporting mesenchymal cells. Previously, such interactions were facilitated by seeding dental mesenchymal cells into poly(epsilon-caprolactone)/ poly (lactide-co-glycolide) (PCL/PLGA) wet electro spun scaffolds, and simultaneously or subsequently seeding dental epithelial cells on the surface in absence of the addition of growth factors [4]. These scaffolds provided a three-dimensional environment to support dental cell attachment, migration, proliferation and/or

differentiation [5, 6]. Moreover, the use of an appropriate scaffold could ensure the morphologically correct shape of the bioengineered tooth, which remains unattainable using scaffold-free methods. However, the current main challenge in any *in vitro* approach for tooth engineering is how to regenerate an adequate epithelial cell layer and sufficient quantities of enamel-like tissue. While odontoblasts remain viable during the life of a tooth, ameloblasts undergo apoptosis prior to tooth eruption [7]. Furthermore, enamel is not only very highly mineralized (>96% of hydroxyapatite), but also consists of a highly complex, hexagonal honeycomb like, crystalline lattice organization, which is extremely strong and able to withstand the significant and variable oral forces of chewing [8]. Therefore, *in vitro* formed enamel required proper dental epithelial cell proliferation and differentiation, and the ability to form an elaborate mineralized enamel matrix.

Many studies have focused on how best to increase the mineralization potential of (stem)cells. For instance, a recent study by Fujioka-Kobayashi et al. demonstrated a significant increase in the total mineralized tissue volume of calvarial defects after the addition of Emdogain, an enamel matrix derivative (EMD) originating from unerupted porcine tooth buds [9] [10]. Another investigation characterized the functional mineralization potential of

three bio inductive materials for vital pulp therapies – Emdogain, MTA (Mineral Troxide Aggregate) and Biodentine. In this study, Emdogain showed highest cell viability, osteo- and odonto-induction capacity [11]. Although these and many more studies showed an enhanced mineralization potential of EMD in relation to bone and or pulp regeneration therapy, EMD has not yet been used in TERMD approaches that focus on the mineralization potential of dental epithelial cells.

Another potential approach to enhance enamel formation could be the addition of Insulin-like growth factor I (IGF-I). IGF-I is present during the differentiation stages of ameloblasts, most abundantly during the secretory stage, and IGF-1 expression is not detectable in maturation stage ameloblasts [12]. A three-year Japanese follow up study of epidemiological data by Kouda *et al.* indicated that higher serum levels of IGF-1 resulted in higher bone mineral acquisition in children [13]. Extrapolating this data, it could be assumed that IGF-1 might influence the mineralization potential in tooth engineering in a similar way.

Therefore, the purpose of the current study was to investigate the effect of EMD and IGF-I on the mineralization potential of dental epithelial cells in a three-dimensional PCL/PLGA wet electro spun scaffold model. We hypothesized that bioengineered three-dimensional mineralized enamel formation could be achieved

by seeding porcine dental epithelial (pDE) cells onto these scaffolds, and that the addition of IGF-I and Emdogain would result in superior osteogenic – odontogenic and ameloblast - differentiation.

Material and Methods

Electrospun scaffolds

The scaffolds were chosen based on earlier experiment with the same cells [4]. The electrospinning solution consisted of PCL (75%, 0.12g/ml) and PLGA 85/31(25%, 0.12 g/ml), both dissolved in liquid 222-Trifluorethanol (TFE, Sigma Aldrich, Zwijndrecht, the Netherlands). The polymers were fully dissolved by magnetic stirring overnight. The syringe, filled with solution, was vertically installed (together with the blunt-end 18G nozzle) in the electrospinning machine (ES-2000S, Esprayer, Tokyo, Japan). The fibers forming the three-dimensional scaffolds were collected in a 96% ethanol bath (surface covered in aluminum foil). The distance between the nozzle and the ethanol was adjusted to 20 cm. The voltage was set at 25.0 kV and a 25 μ l/min feeding rate was used. The scaffolds were collected from the ethanol bath after 5 minutes and stored at -80°C for 60 minutes before freeze-drying (VirTis BenchTop Pro, SP scientific, Pennsylvania, USA) overnight. Thereafter, scaffolds were cut with a 6mm disposable biopsy punch (Kai medical, Solingen, Germany) and stored at -80°C until use. Before use, scaffolds were

sterilized and made hydrophilic by Radio Frequent Glow Discharge Treatment (RFGD-T; Harrick Plasma Cleaner/ Sterilizer, Harrick plasma, Ithaca, USA)[14].

Cell culture

Cryopreserved pDE [4] cells were recovered (Passage 1) and cultured with epithelial cell media [LHC-8 #12678-017 (Gibco, Bleiswijk, The Netherlands) containing 10% FBS, 1% PSA (penicillin/streptomycin/amphotericin), and 0.5 μ g/ml epinephrine]. The medium was refreshed every 2-3 days. Once \geq 95% confluence was reached, pDE cells were seeded into 12-well Upcell thermo-responsive plates (Thermo Scientific, Netherlands) at a cell seeding density of 1.6×10^6 cells per 12-well Upcell ($=3.5\text{cm}^2$)[15]. Non-seeded cells were collected to serve as a Day 0 value for RNA isolation (~20 million total). The pDE cells were grown in Upcell thermo-responsive wells for ~7 days until confluent.

Human Dental Pulp Stem Cells (hDPSCs, P3) [4] were retrieved from cryopreservation approximately one week after the pDE cells were thawed to ensure that both types of cells would reach confluence at the same time. Human cells were used from discarded M3 teeth, following national guidelines for working with human materials, and did not require further ethical committee approval. Upon reaching confluence, hDPSCs were statically seeded onto scaffolds

at 2.0×10^5 cells per scaffold, in hDM cell media [Advanced DMEM/F12 #12634 (GIBCO) containing 10% FBS, 25 μ g/ml ascorbic acid, 1% Glutamax, 1% PSA], and refreshed every 2-3 days. Both pDE and hDM cells were cultured at 37°C in a humidified 5% CO₂ atmosphere.

Construct preparation

After 7 days *in vitro* culture, hDM-seeded scaffolds and pDE cell sheets (pDE-CS) were combined as follows. First, media was removed from the hDPSC seeded scaffolds to facilitate the attachment between the scaffolds and pDE-CS. The hDM seeded scaffolds were then transferred to Upcell 12-well plates containing pDE cell sheets. Four scaffolds were transferred to each well. Then 160 μ l (40 μ l/ scaffold) of specific, group assigned, medium (see below) was added per well to prevent drying. After a 30 minutes' incubation period to ensure attachment between the hDM seeded scaffold and pDE cell sheet, the medium was supplemented to 250 μ l, and finally after 7 days in vitro culture to 500 μ l. 250 μ l of the medium was refreshed daily. Three groups were examined and all groups were a mixture of DM medium and DE medium (1:1):

- 1- DM/DE normal medium (NM; 1:1, control group)
- 2- DM/DE medium (1:1) with 100 μ g/ml IGF-1
- 3- DM/DE medium (1:1) with 200 ng/ml EMD

Samples were harvested and fixed at days 3, 14 and 21.

For CS detachment, media was aspirated and 50 µl/well of fresh media was added to prevent dehydration during the detachment procedure (according to manufacturer's instructions) [16]. The samples were placed at room temperature (24°C) for ±30 minutes until detachment from the Upcell plates was visually observed. The cell sheet edges were loosened with a needle and split in 4 with a scalpel under the dissecting microscope (ZEISS SteREO Discovery. V8, Pleasanton, USA). Each scaffold was then wrapped with an epithelial CS and transferred on top of filter paper in a new 12 well plate, positioning them so that the dental epithelial CS was positioned on top of the hDPSC seeded scaffold. After the appointed time points in culture, samples were harvested, fixed in formalin ON at 4°C and stored in PBS until further processing.

Histological staining (H&E)

Fixed constructs were embedded in OCT, serially sectioned at six microns (Leica RM 2135, Leica, Bannockbur/Illinois, USA), mounted using a Premiere Tissue Floating Bath XH-1001 and slide warmer (Premiere XH-2001, C&A Scientific, Virginia, USA) set to 45°C for the first 60 minutes, and then increased to 54°C overnight.

Samples were rehydrated in Xylene and ethanol series, stained with Hematoxylin for 1 minute, rinsed in water and diluted hydrochloric acid water, ammonia water, and stained with Eosin for 20 seconds. Samples were dehydrated in ethanol series and xylene, and mounted using Permount medium (Fisher Scientific, Illinois, USA). Micrographs were made with a Zeiss Axio Imager/ Z1 equipped with digital Zeiss Axiocam HRC camera (Zeiss, Pleasanton, USA).

Immunofluorescent (IF) Analyses

IF staining was performed to visualize hDM and pDE cell-cell interactions. The primary antibodies included: anti-Vimentin (VM, Mouse, 1:50), anti-Ecad (Rabbit, 1:50) and anti- β -integrin 1 (Mouse, 1:25). Secondary antibodies included Goat Anti-Mouse (Excitation: 568nm, Cy5), Goat Anti-Mouse (Excitation: 488nm, green), Goat Anti-Rabbit (Excitation: 652nm, Cy5, with 4',6-diamidino-2-phenylindole (DAPI, blue) counterstain. Porcine tooth bud sections were used as positive controls for primary antibodies Ecad and VM, and human dental pulp was used as positive control for Integrin. Samples lacking the primary antibody were included as negative controls. IF staining color's intensity fluctuates for the different groups yet is positively present in all.

Scanning Electron Microscope (SEM) analysis

SEM was executed to visualize the status of mineralization and to monitor cell growth in harvested 3, 14 and 21 day samples. Samples were washed in PBS, fixed with 2.5% Glutaraldehyde (pH 7.31), post fixed with 1% Osmium Tetroxide for 1 hour on ice, dehydrated in a series of Ethanol, and air dried in tetramethylsilane. Samples were sputter coated twice with 10nm Chromium (Q150T S, Quorum technologies, Lewes, UK). Images were taken in a Zeiss Gemini sigma 300 Scanning Electron Microscope (Zeiss, Oberkochen, Germany).

RNA isolation and quantitative Real-Time Polymerase Chain Reaction (qRT-PCR) analyses

QRT-PCR was performed to monitor cell differentiation marker expression in D0 and D21 construct samples. Four scaffolds per group were pooled to ensure that sufficient amounts of RNA were obtained. Control 2D cultured hDM and pDE cells were trypsinized, lysed in β -Mercaptoethanol Cell Suspension (Trizol), and preserved at -80°C until processing. The scaffolds were dissociated into small pieces using RNase treated scissors, and the RNA extraction was performed using the RNeasy Mini Kit (Qiagen sciences, Baltimore, USA). The RNA yield was confirmed with a spectrophotometer (Nanodrop 1000, Thermo Scientific). Reverse Transcription was carried out with the SuperScript First-Strand Synthesis system (Invitrogen, Thermo Scientific), and cDNA yield was

determined using a spectrophotometer. The qRT-PCR was executed using the Protocol for Real Time PCR with the Stratagene MX3000P (Stratagene, San Diego, California). The primers, as displayed in table 1, (1 µl each) used were hDSPP, GAPDH (control primer), hBGLAP and pAMBN (Qiagen sciences, Baltimore, USA). All three media conditions were tested with all primers in triplicate.

Statistical analysis

All data were presented as mean ± Standard Error. Statistically significant values were defined as $p \leq 0.05$ based on one-way analysis of variance (ANOVA) and post hoc Tukey testing.

Results

Histological staining

cells dispersedly evenly throughout the scaffolds, and covered by a pDE-CS. The 3 day pDE-CS constructs showed evidence of fragmentation likely due to handling. On Days 14 (Figure 1 D-F) and 21 (Figure 1 G-I) the interstitium between the scaffold fibers appeared to be filled with hDM cells, and the cell sheets were in close contact with the scaffolds and had remained largely intact. The cell sheet thickened over time, by visual

Table 1: Overview of the four used primers for the qRT-PCR analyses and their origin/catalog numbers.

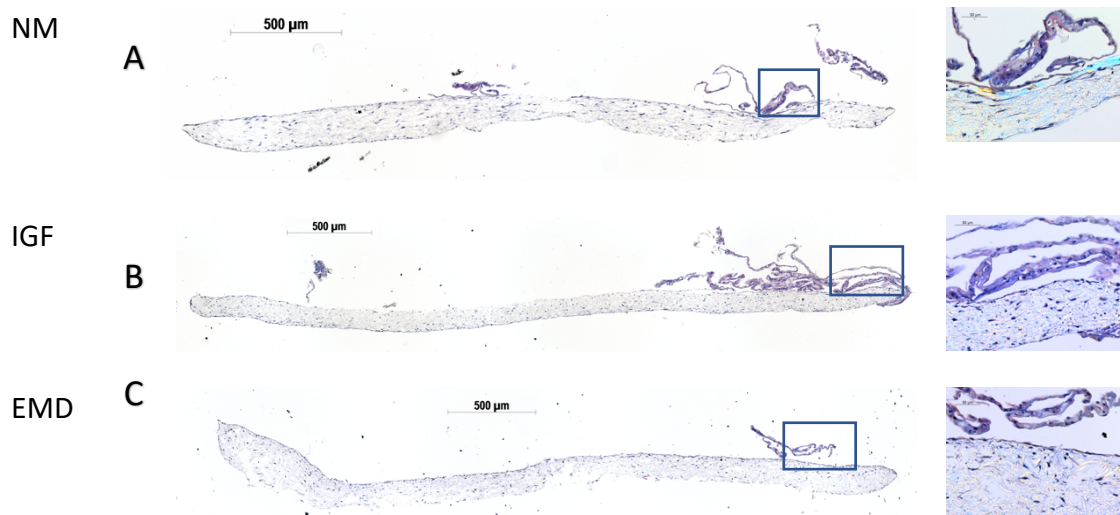
Primer (1 µl):	Catalog number:
hDSPP	PPH57747E-200
GAPDH (control primer)	PPH00150F-200
hBGLAP	PPH01898A-200
pAMBN	PPS00441A-200

Day Full image 10x
3

Dental cell-distribution throughout the scaffolds was investigated using histological analysis. At day 3 (Figure 1A-C), all scaffolds showed the presence of hDM

inspection most evidently the IGF-I group. The epithelial polygonal shaped cells multiplied in the days following the experiment while remaining on top of the scaffolds, not migrating inwards. The mesenchymal cells multiplied as well.

Detailed polarized image 40x



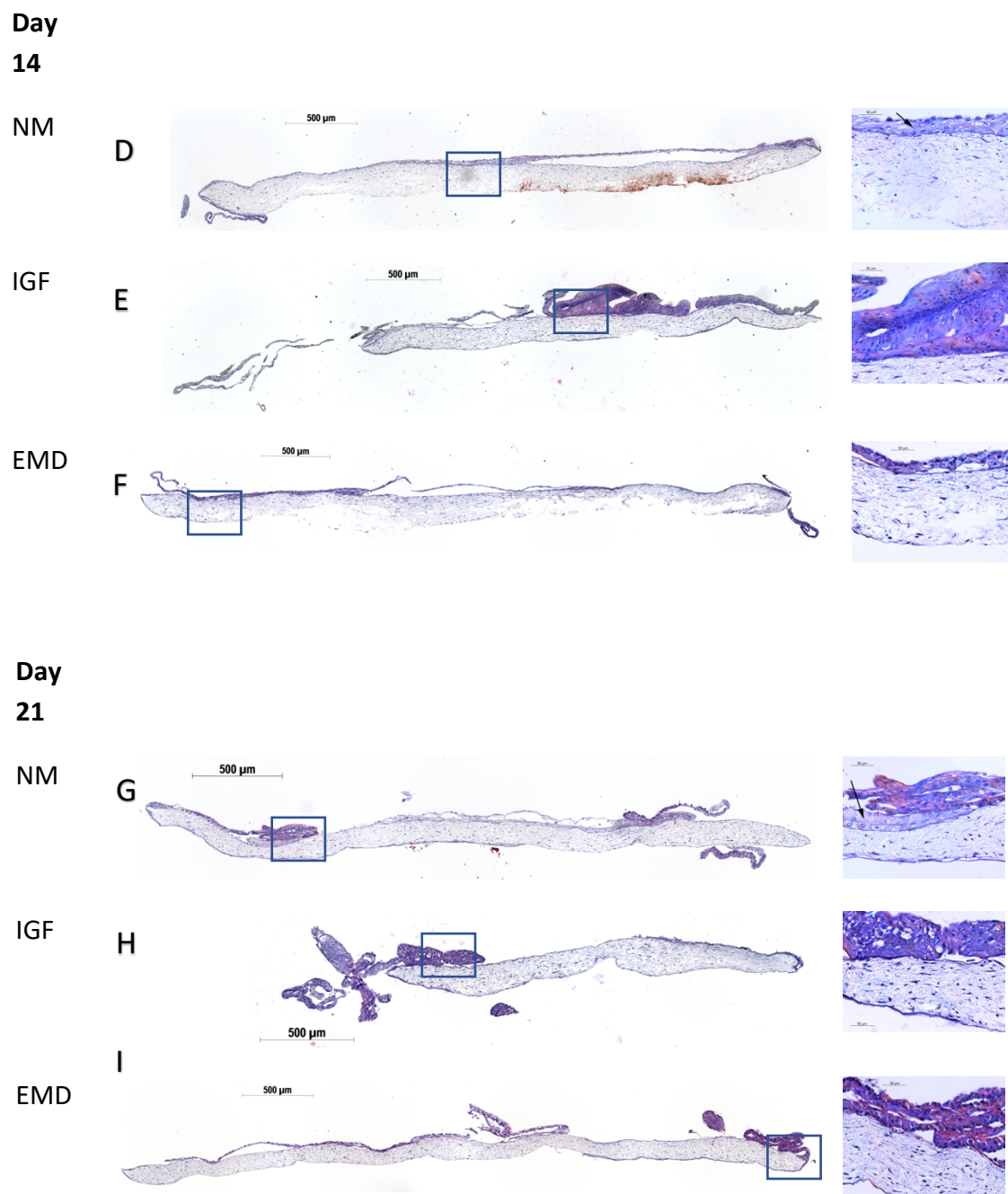


Figure 1. Cell seeding procedure assessed with histological staining. H&E stained sectioned scaffolds cultured with HDM cells and pDE cells for 3 (A-C), 14 (D-F) and 21 (G-I) days in normal medium (A, D & G), medium supplemented with IGF-I (B, E & H), and EMD (C, F & I) enriched medium. For each sample, low magnification (10x, scale bar = 500 μ m) image provides the overview to monitor cell-growth and visualize the cell-distribution within the scaffold. The high magnification polarized images (40x; inserts) demonstrate the presence of both dental epithelial as mesenchymal cells, as well as mineralized tissue ECM polarized structures particularly evident in NM D14 (D) and NM D21 (G)(arrows)

Immuno-Fluorescent staining (IF)

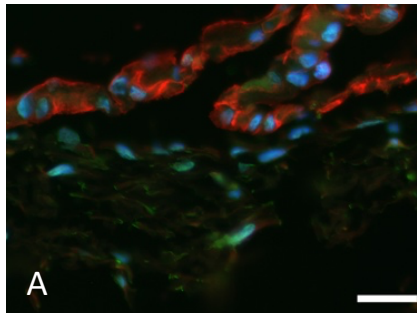
To visualize the distribution of cells (Figure 2), epithelial cells were stained for Ecad, and hDPSCs for Vimentin. hDPSCs were seen all

through the sample. The IF images corroborated the H&E staining, with pDE cells maintaining the cultured cell sheet shape, whereas the hDM cells were evenly distributed throughout the sample. To visualize

hDM-pDE cell contacts, IF imaging for β -integrin 1 was performed (Figure 3). If results showed the formation of hDM-pDE cell contacts at all time points, in all three types of media.

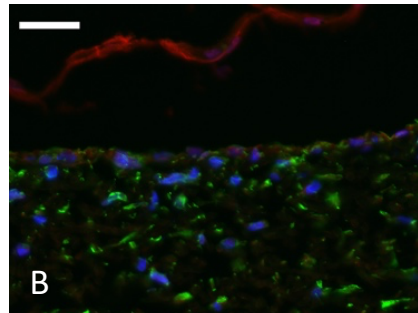
VM&Eca NM
d (1:50,
40X)

Day 3



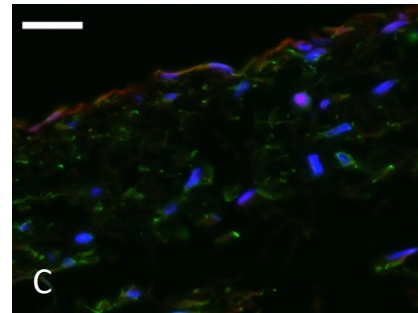
A

IGF-1



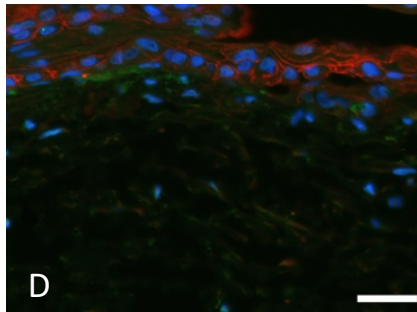
B

EMD

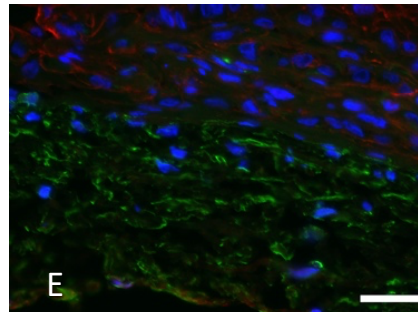


C

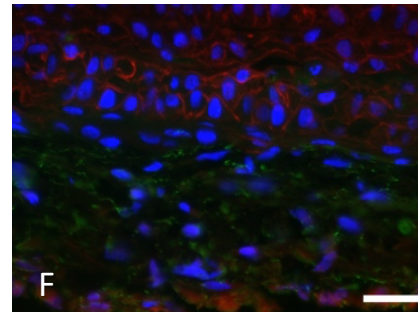
Day 14



D

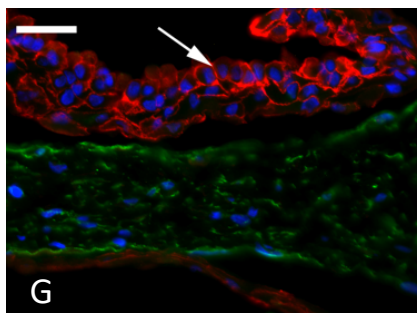


E

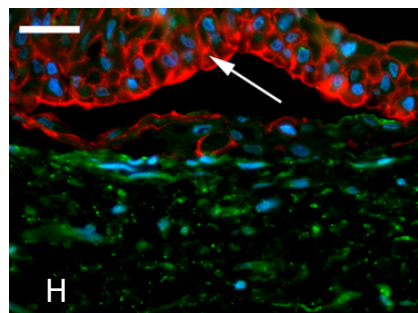


F

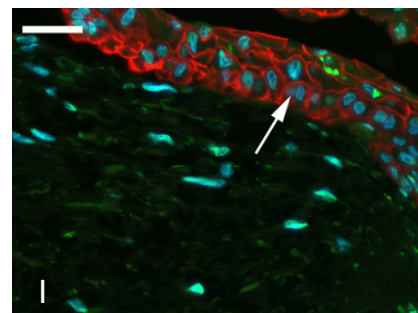
Day 21



G



H



I

Figure 2. Location and interactions of dental cells as assessed by immunofluorescent staining. Immunofluorescent staining at Days 3 (A-C), 14 (D-F) and 21 (G-I) in NM (A, D & G), IGF-1 (B, E, H) and EMD (C, F & I). DAPI (blue) was used to counterstain all nuclei. Vimentin (green) labels hDM cells, while Ecad (red) labels pDE-CSs. Very close contact between the different layers was observed in all constructs (scale bar = 50 μ m). Distinguished polarized structures are clearly visible in the D21 samples (arrows)

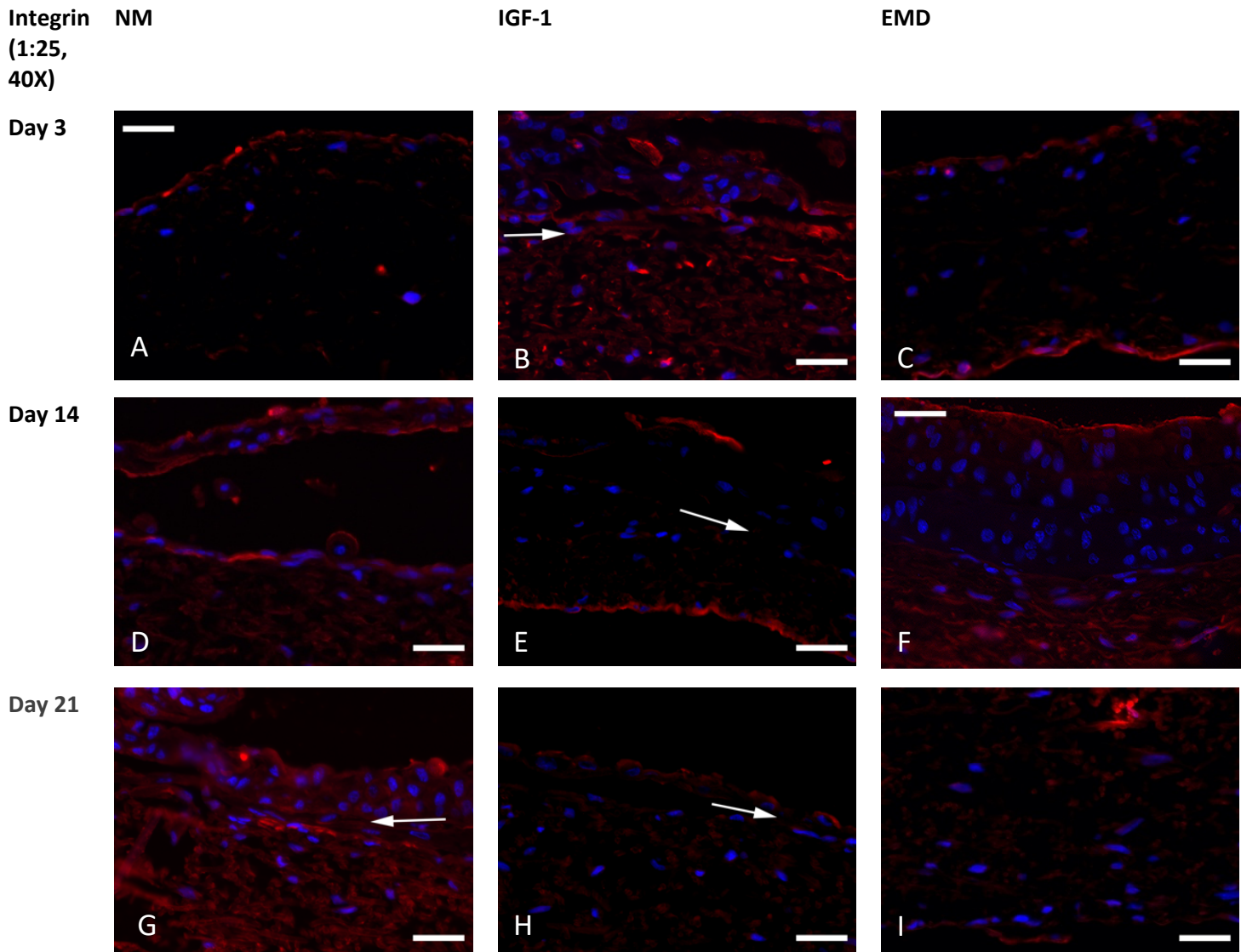


Figure 3. Location and interactions of dental cells as assessed by immunofluorescent staining. Immunofluorescent staining for anti-integrin 1 (red) at Days 3 (A-C), 14 (D-F) and 21 (G-I) in constructs cultured in NM (A, D & G), IGF-1 (B, E, H) and EMD media (C, F & I). Note the abundant cell-cell contact between pDE and hDM cells throughout several of the constructs (arrows)(scale bar = 50 μ m)

Scanning Electron Microscopy (SEM)

The scaffold, hDM-DE cell morphology, mineralized dental matrix formation were assessed using SEM. In the NM group (Figure 4A, D & G) the pDE-CS was clearly observed, with no obvious differences in pDE

cell morphology over time. A similar result was observed in the IGF group (Figure 4B, E & H), where a pDE-CS covering the hDM cell seeded scaffold was clearly observed, with no obvious difference over time in culture. In contrast, the EMD group (Figure 4C, F

& I) showed a markedly different appearance, in that the pDE-CS transparency decreased over time, and the hDM seeded scaffold surface structure exhibited a complex, honeycomb like, crystalline lattice organization at D21 (Figure 4I).

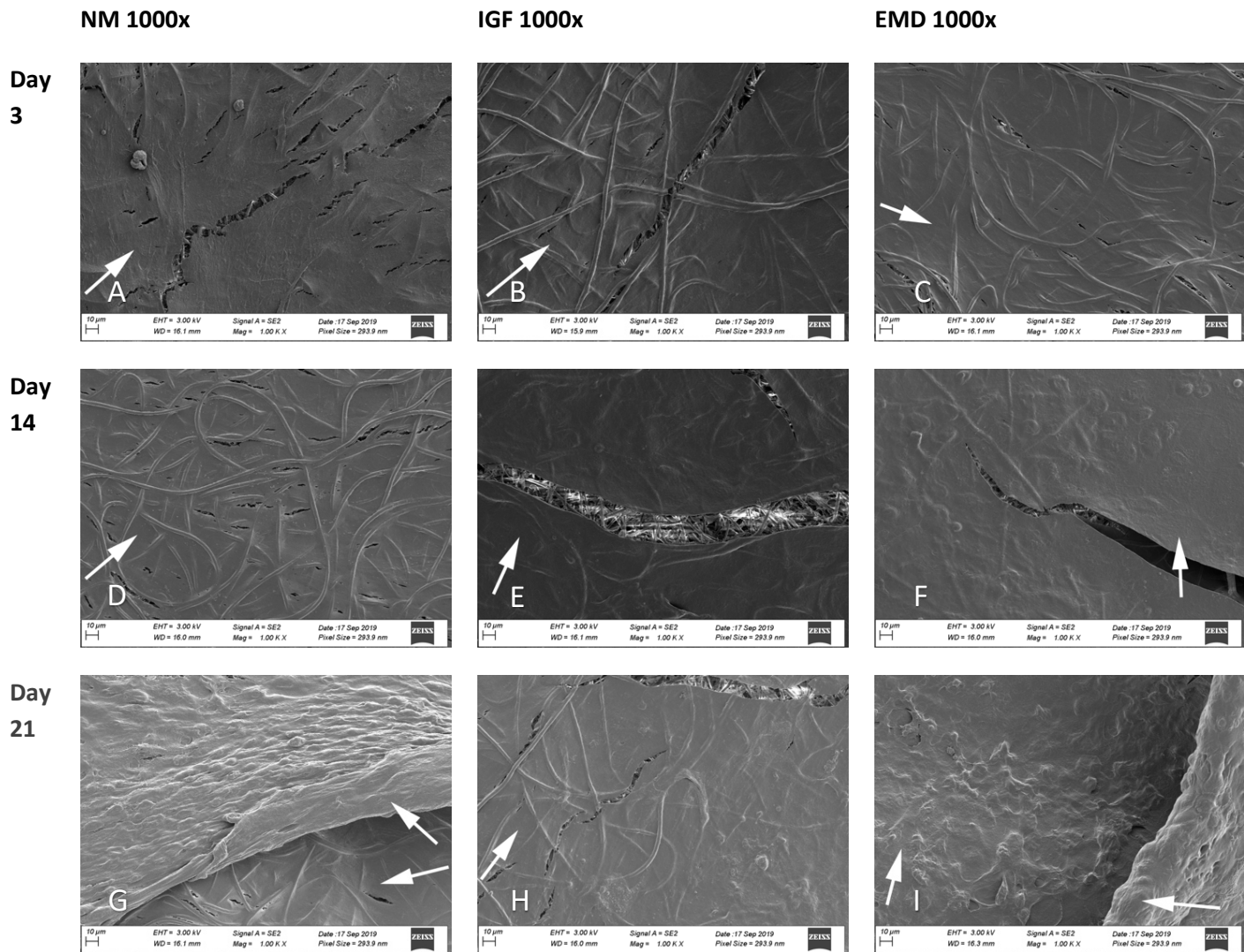


Figure 4. SEM imaging of dental epithelial cell sheets. SEM imaging of in vitro cultured bioengineered tooth bud constructs at days 3 (A-C), 14 (D-F) and 21 (G-I), in the NM (A, D & G), IGF (B, E & H) and EMD (C, F & I) culture conditions (1000x magnification). All images show a clearly visible DE cell sheet (arrows). The arrows in the SEM images are pointing at a small piece of the visible DE cell sheet, to evidence that the sheet obviously spreads across most of the image (apart from small cracks, most likely due to fragmentation/ human handling). The surface structure of the EMD treated group portrays a complex honeycomb (hexagonal crystallized (clear deposition of minerals) structures, depicting the external likes of a beehive) like crystalline lattice organization at D21(I) as compared to D3(C)

Quantitative Real-Time Polymerase Chain Reaction (qRT-PCR)

qRT-PCR analyses of dental cell differentiation marker expression were performed (Figure 5). The expression of the ameloblast differentiation marker AMBN was significantly higher in the IGF-1 and Emdogain groups as compared to the NM group ($P<0.05$). No significant differences in the expression of DSPP and OC were observed.

pharmaceutical or regenerative medicinal approaches. This study showed the construction of a multi-dimensional scaffold-dental epithelial cell sheet-based model, and the utility of this model to demonstrate the positive effects on mineralization potential of IGF-1 and Emdogain.

In hindsight, the 21-day period of time is not long enough for considerate in vitro mineralized tissue formation. Future research could incorporate the use of Alizarin Red S staining or EDS SEM analysis to

used PCL/PLGA in tissue engineering approaches on this matter.

Of note, several technical issues were encountered. One concerned the static seeding method used to seed hDPSCs onto the electrospun scaffold. Based on literature, it might be argued that a dynamic cell seeding method would be a better method [19], as rotational seeding leads to a more even distribution of cells, especially in the deep interstitium of porous carrier materials. On the other hand, rotational seeding approaches

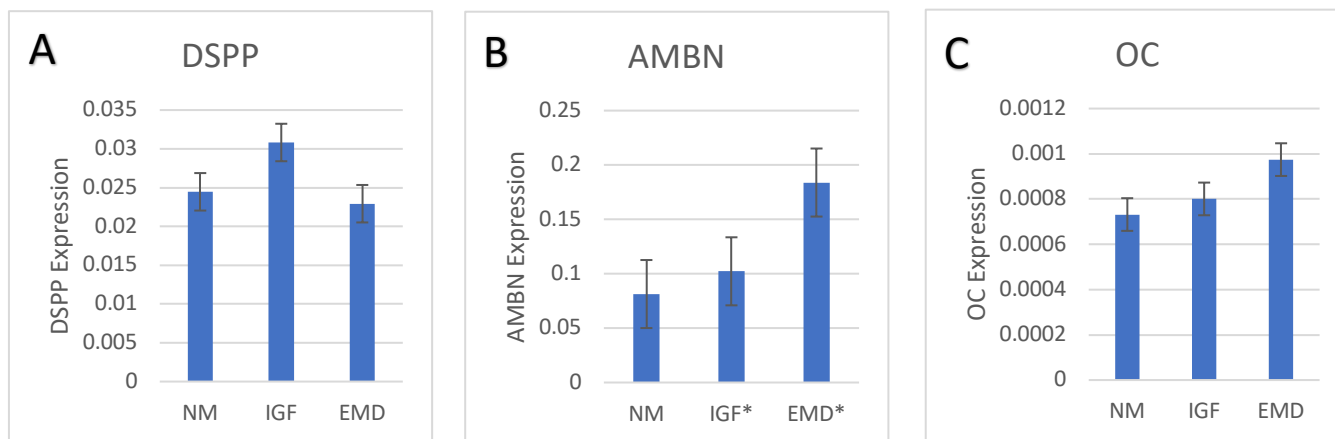


Figure 5. qPCR analyses of dental cell differentiation marker expression. Expression of (A) DSPP (B) AMBN(C) BGLAP/OC as normalized to D0 dental cell cultures. The expression of the ameloblast differentiation marker AMBN was significantly higher in the IGF-1 and Emdogain treated groups as compared to the NM group ($P<0.05$). No significant differences in the expression of DSPP and OC were observed

Discussion

Dental tissue damage remains a considerable health concern in our current society. The ability to regenerate organic, vital tooth material would be highly desirable to enable future therapeutic options. Moreover, cultured mineralized tooth-like tissue could serve as an *ex vivo* screening tool for novel

determine Ca^{2+} deposition on the scaffolds.

The PCL/PLGA scaffolds were assumed not to exhibit parameters such as an increased cytotoxicity and/or genotoxicity potential due to scaffold degradation. The material is believed to be biocompatible based on multiple experiments [17, 18] that

might also damage or present undesirable mechanical cues to the cells. Our results indicated that static seeding of hDM cells on the surface, directly adjacent to where the cell sheet would be placed, apparently was sufficient for the current scaffold dimensions used in this study. Furthermore, the results showed an adequate enough amount of cell

distribution for the research to be executed.

Another technical aspect was the choice of how best to combine the hDM seeded scaffold with the epithelial cells, after these epithelial cells had been grown separately as confluent sheets. This approach was based on the assumption that DE cells have the tendency to form coherent monolayers, as shown before in a study performed by Seo et al. [20] and by our group [15]. Our results indeed confirmed the assumption that pDE cells formed polarized monolayers, and that the cell sheet technology was accommodating for the purpose of making layered constructs with distinct cellular phenotypes. Still, a certain amount of fragmentation of the epithelial cell sheets occurred, shown in the histological images of day 3 constructs, raising a concern towards the applied model, although such fragmentation likely occurred as a result of manual handling during the harvesting. The day 3 samples proved quite challenging to collect due to their extremely fragile nature after culture for such a short period of time. Although no damage was visible by eye during the construct harvest, it was clearly observed in harvested and sectioned specimens examined via light microscopy. At later timepoints, the constructs appeared more robust, as more rigid sheets could be formed, and no fragmentation occurred anymore. Future research could explore the different methods for

adapting the scaffold structure to make it less susceptible to fragmentation in early stages. A study performed by Hong et al. describes different biomaterials that could be considered [21] to possibly enhance the handling efficiency and minimize fragmentation.

Although our results clearly showed that IGF-1 and EMD exhibited positive and significant effects on dental cell differentiation, in most of the constructs analyzed as evidenced by q-PCR, the expression levels of DSPP and OC were not affected. This may be due to the relatively low cell seeding density used, and/or in combination with the limited *in vitro* culture time frame. At later timepoints, increased amounts of mineralized dental matrix were observed via light and SEM microscopical analyses. As such, a longer experimental time frame would be advisable for future research when regarding specifically the expression of mineralized tissue markers.

When comparing these results to the published literature, certain discrepancies are noteworthy. For instance, Grandin et al. recently reviewed the *in vitro* cellular effects of Emdogain, showing that in periodontal ligament and osteoblastic cells, Emdogain enhanced cell proliferation, gene expression, protein production, and differentiation [22]. Also, angiogenesis was shown to be stimulated by EMD in this study [22].

However, for epithelial cells specifically, a cytostatic tendency was described. This is in contrast with our results which showed normal unhindered growth and enhanced effect on the mineralization potential of dental epithelial cells. Our results are supported by published literature including that of Qu et al., who investigated the effects of Emdogain on the proliferation and migration of human oral epithelial cells [23]. This study concluded that the addition of EMD resulted in significant enhancement of the proliferation and viability of the epithelial cells [18]. However, this study used a 2D model and did not assess the mineralization of treated epithelial cells. Likewise, a recent study by Li et al. showed that IGF-1 facilitated odontogenesis of cultured periodontal ligament stem cells [24], which again corroborated the data for our differentiated epithelial and dental mesenchymal cell co-cultured constructs. In summary, our hypotheses were validated in this study, which demonstrated that both Emdogain and IGF-I are important for the enhancement of dental cell differentiation and proliferation in our system.

Conclusion

Based on the results of this study, we conclude that a multi-layered three-dimensional tooth bud model was successfully created by combining hDPSC-seeded scaffolds with dental epithelial cell sheets. This multi-

layered bioengineered 3D tooth bud model exhibited abundant hDM-pDE cell-cell contact and was sufficient to support pDE and hDPSC cell proliferation and differentiation. In particular, the addition of IGF-1 and EMD increased the mineralization potential of the pDE cells. Future research is therefore justified and warranted to further verify these conclusions in a preclinical *in vivo* model.

Acknowledgements

Radboud Honours Programme Medical Sciences (Radboud Honours Academy, Nijmegen), Associatie Nederlandse Tandartsen (ANT), Radboud UMCN student grant, NIH/NIBIB R01 DE026731 (PCY).

Disclosure of potential conflict of interest

The authors designated no potential conflict of interest.

References

1. Global, Regional, and National Prevalence, Incidence, and Disability-Adjusted Life Years for Oral Conditions for 195 Countries, 1990-2015: A Systematic Analysis for the Global Burden of Diseases, Injuries, and Risk Factors. Kassebaum NJ, Smith AGC, Bernabe E, Fleming TD, Reynolds AE, Vos T, et al. J Dent Res. 2017;96(4):380-7.
2. Caries Management - Science and Clinical practice. In: Effenberger DS, editor. Hendrik Meyer-Leuckel SP, Kim R. Ekstrand. Stuttgart New York: Thieme; 2013. p. 8,9.
3. The replacement of missing teeth. Canadian family physician Medecin de famille canadien. Zarb GA. 1988;34:1435-40.
4. Influence of highly porous electrospun PLGA/PCL/nHA fibrous scaffolds on the differentiation of tooth bud cells *in vitro*. Journal of biomedical materials research Part A. Cai X, Ten Hoopen S, Zhang W, Yi C, Yang W, Yang F, et al. 2017;105(9):2597-607.
5. Electrospinning approaches toward scaffold engineering--a brief overview. Artificial organs. Boudriot U, Dersch R, Greiner A, Wendorff JH. 2006;30(10):785-92.
6. The influence of electrospun fibre scaffold orientation and nano-hydroxyapatite content on the development of tooth bud stem cells *in vitro*. Odontology. van Manen EH, Zhang W, Walboomers XF, Vazquez B, Yang F, Ji W, et al. 2014;102(1):14-21.
7. Dental tissue regeneration - a mini-review. Gerontology. Yen AH, Yelick PC. 2011;57(1):85-94.
8. Advances and perspectives in tooth tissue engineering. Journal of tissue engineering and regenerative medicine. Monteiro N, Yelick PC. 2017;11(9):2443-61.
9. Straumann.com [Available from: <https://www.straumann.com/en/dental-professionals/products-and-solutions/biomaterials/biologics.html>].
10. Effect of enamel matrix derivative liquid in combination with a natural bone mineral on new bone formation in a rabbit GBR model. Clin Oral Implants Res. Kobayashi E, Fujioka-Kobayashi M, Saulacic N, Schaller B, Sculean A, Miron RJ. 2019;30(6):542-9.
11. Response of stem cells from human exfoliated deciduous teeth (SHED) to three bioinductive materials - An *in vitro* experimental study. Dahake PT, Panpaliya NP, Kale YJ, Dadpe MV, Kendre SB, Bogar C. Saudi Dent J. 2020;32(1):43-51.
12. Expression and regulation of insulin-like growth factor-I in the rat incisor. Growth Factors. Joseph BK, Savage NW, Young WG, Gupta GS, Breier BH, Waters MJ. 1993;8(4):267-75.
13. Associations between serum levels of insulin-like growth factor-I and bone mineral acquisition in pubertal children: a 3-year follow-up study in Hamamatsu, Japan. J Physiol Anthropol. Kouda K, Iki M, Ohara K, Nakamura H, Fujita Y, Nishiyama T. 2019;38(1):16.
14. [Effect of radio frequency discharge plasma on surface properties and biocompatibility of polycaprolactone matrices]. Biomed Khim. Bolbasov EN, Antonova LV, Matveeva VG, Novikov VA, Shesterikov EV, Bogomolova NL, et al. 2016;62(1):56-63.
15. Dental cell sheet biomimetic tooth bud model. Biomaterials. Monteiro N, Smith EE, Angstadt S, Zhang W, Khademhosseini A, Yelick PC. 2016;106:167-79.
16. Scientific TF. [Available from: <https://assets.thermofisher.com/TFS-Assets/LSG/manuals/D17402.pdf> E.
17. Design, synthesis, characterization, and cytotoxicity of PCL/PLGA scaffolds through plasma treatment in the presence of pyrrole for possible use in urethral tissue engineering. J Biomater Appl. Sánchez-Pech JC,

- Rosales-Ibáñez R, Cauich-Rodriguez JV, Carrillo-Escalante HJ, Rodríguez-Navarrete A, Avila-Ortega A, et al. 2020;34(6):840-50.
18. Biocompatibility of PCL/PLGA-BCP porous scaffold for bone tissue engineering applications. *J Biomater Sci Polym Ed.* Thi Hiеп N, Chan Khon H, Dai Hai N, Byong-Taek L, Van Toi V, Thanh Hung L. 2017;28(9):864-78.
19. Static versus vacuum cell seeding on high and low porosity ceramic scaffolds. *Journal of biomaterials applications.* Buizer AT, Veldhuizen AG, Bulstra SK, Kuijer R. 2014;29(1):3-13.
20. Epithelial monolayer culture system for real-time single-cell analyses. *Physiological reports.* Seo JB, Moody M, Koh DS. 2014;2(4):e12002.
21. Cell-Electrospinning and Its Application for Tissue Engineering. *Int J Mol Sci.* Hong J, Yeo M, Yang GH, Kim G. 2019;20(24).
22. Enamel matrix derivative: a review of cellular effects in vitro and a model of molecular arrangement and functioning. *Tissue Eng Part B Rev.* Grandin HM, Gemperli AC, Dard M. 2012;18(3):181-202.
23. Effect of Emdogain on proliferation and migration of different periodontal tissue-associated cells. *Oral Surg Oral Med Oral Pathol Oral Radiol Endod.* Qu Z, Laky M, Ulm C, Matejka M, Dard M, Andrukhover O, et al. 2010;109(6):924-31.
24. Odontogenesis and neuronal differentiation characteristics of periodontal ligament stem cells from beagle dog. *J Cell Mol Med.* Li X, Liao D, Sun G, Chu H. 2020;24(9):5146-51.